*Materials Transactions*, Vol. 54, No. 6 (2013) pp. 879 to 883
Special Issue on Nanojoining and Microjoining

# Metal–Metal Bonding Process Using Cu+Ag Mixed Nanoparticles

Jianfeng Yan[1], Guisheng Zou[1], Yingchuan Zhang[1], Jiaxin Li[1],
Lei Liu[1], Aiping Wu[1] and Y. Norman Zhou[1,2]

[1]*Department of Mechanical Engineering, Tsinghua University & Key Laboratory for Advanced Materials Processing Technology, Ministry of Education of China, Beijing 100084, P. R. China*
[2]*Centre for Advanced Materials Joining, Department of Mechanical and Mechatronics Engineering, University of Waterloo, 200 University Avenue West, Waterloo, ON, N2L 3G1, Canada*

The Cu+Ag mixed nanoparticles were prepared based on the chemical reduction method. The polymer coated on the Cu+Ag mixed nanoparticles can protect Cu nanoparticles from oxidation. The metal–metal joint of silver plated Cu bulks was investigated with the use of Cu+Ag mixed nanoparticles. The bonding experiments show that joint with shear strength about 20 MPa was formed at the bonding temperature above 250°C under 5 MPa using Cu+Ag mixed nanoparticles. The strength of bonding using Cu+Ag mixed nanoparticles is lower than that of bonding using pure Ag nanoparticles. This may be due to the fact that the sintering between the Cu nanoparticles and Ag nanoparticles is more difficult than the sintering between Ag nanoparticles. [doi:10.2320/matertrans.MD201222]

(Received December 17, 2012; Accepted February 25, 2013; Published May 25, 2013)

**Keywords:** *copper+silver mixed nanoparticles, sintering, bonding, electronics packaging*

## 1. Introduction

Tin-lead solders have been widely used as bonding materials in the electronics industry for many years. However, since the lead contained in the solders do harm to natural resources and human health, legislation has proposed to limit the use of lead in solders in many countries.[1)] This situation has stimulated substantial research and development efforts to discover alternative lead-free solder alloys, including Sn–Zn, Sn–Cu, Sn–Bi, Sn–Ag systems.[2,3)] There are still some drawbacks that limit extensive applications of lead-free solders, such as high melting temperatures, poor wettability and poor solderability. Especially, there are no suitable lead-free high temperature solders. The high temperature solders containing 90–95 mass% Pb are still widely used in various applications.[4)]

Recently, there has been an increasing focus on low temperature interconnect technologies with metal nanoparticles (Ag nanoparticles, Cu nanoparticles. etc.) as an alternative technique for the soldering with lead.[5–8)] The interconnect technologies have potential application for flexible electronics, including flat-panel display, organic electronics, and low-cost disposable microelectronics devices on plastic substrate;[7–9)] Furthermore, metal nanoparticles provide a promising lead-free, high temperature bonding material alternative.[6,10,11)] Cu+Ag mixed nanoparticles have some advantages such as lower cost and good resistance to electrical migration.[12)] In this study, the metal to metal bonding process using Cu+Ag mixed nanoparticles was studied. The polymer coated on the Cu+Ag mixed nanoparticles can protect them from oxidation. The effects of bonding temperatures and Cu content in the mixed nanoparticles on the bondability were discussed.

## 2. Experimental

Ag nanoparticles was prepared by the polyol method and the following centrifugation as reported previously.[13,14)] The Cu nanoparticles was prepared in ambient atmosphere based on the polyol method.[8)] Cu+Ag mixed nanoparticles with different molar fractions (Cu/Ag molar ratio: Cu, Cu4/Ag1, Cu1Ag1, Cu1Ag4 and Ag) were prepared by mechanical mixing of Cu nanoparticles and Ag nanoparticles.

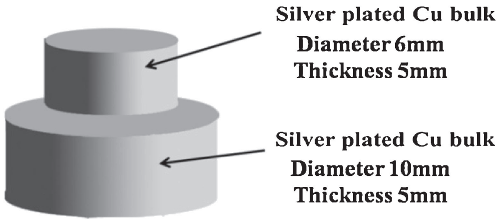

Fig. 1 Schematic illustration of the bonding specimens using Cu+Ag mixed nanoparticles.

The silver plated Cu bulks were bonded using Cu+Ag mixed nanoparticles at 250°C in air under bonding pressure of 5 MPa and held for 5 min. The silver plated copper discs were made by firstly plating a layer of nickel (about 2 µm) on the pure copper discs. Then silver plating (about 4 µm) was applied over the nickel plating. Figure 1 shows the schematic illustration of the bonding specimens. The nanoparticles were applied on the faying surfaces of Φ 6 mm Cu bulk, which was set on the Φ 10 mm Cu bulk. Afterwards, these prepared bonding specimens were heated up to bonding temperature in a resistance furnace in air under 5 MPa.

## 3. Result and Discussion

### 3.1 Characteristics of nanoparticles

Figure 2 shows scanning electron microscopy (SEM) and transmission electron microscopy (TEM) images of Ag nanoparticles and Cu nanoparticles, which were synthesized by chemical reduction method, respectively. Most of Cu nanoparticles and Ag nanoparticles reveal spherically shaped particles. The polymer coated on the surface of metal nanoparticles can be detected on the TEM images, as shown in Fig. 2.[12)] It is assumed that the thin layer polymer

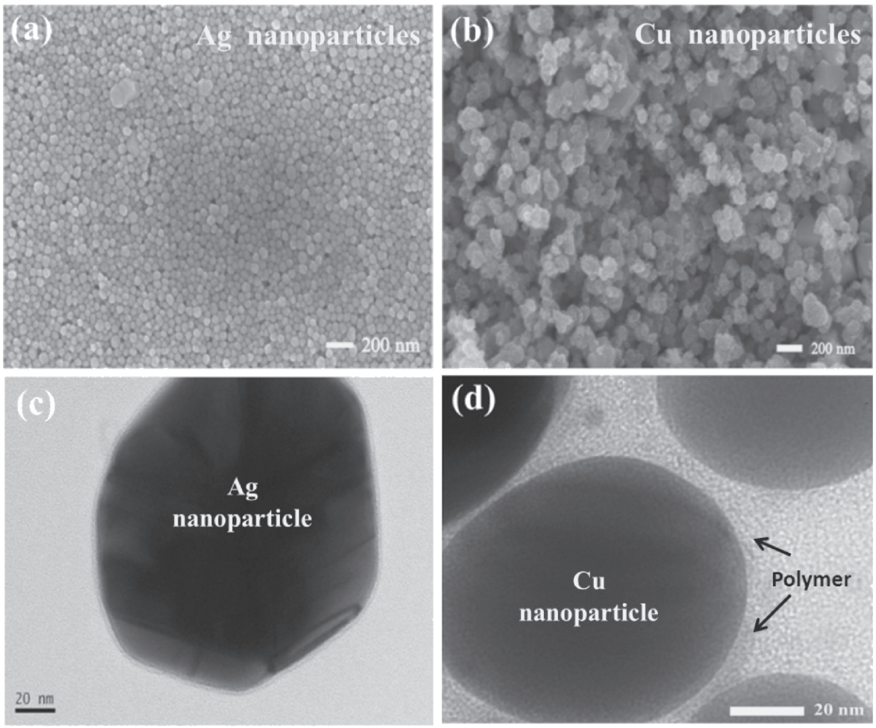

Fig. 2 SEM images of (a) Ag nanoparticles, (b) Cu nanoparticles and TEM images of (c) Ag nanoparticles and (d) Cu nanoparticles.

consisted of polyvinylpyrrolidone can protect Cu nanoparticles from oxidation when heated in air.[8)]

The reduction mechanism of Ag nanoparticles by ethylene glycol probably involves the following chemical reactions:

$$2HOCH_2 - CH_2OH \rightarrow 2CH_3CHO + 2H_2O \quad (1)$$

$$2CH_3CHO + 2AgNO_3 \rightarrow CH_3CO - COCH_3 + 2Ag + 2HNO_3 \quad (2)$$

During the synthesis of Cu NPs, the polyvinylpyrrolidone was used as a protecting agent. Sodium hypophosphite monohydrate ($NaH_2PO_2{\cdot}H_2O$) was used to reduce copper sulfate pentahydrate ($CuSO_4{\cdot}5H_2O$). The copper ions may be reduced by atomic hydrogen evolving from the reaction of hypophosphite with water, as the following chemical reaction:

$$H_2PO_2^- + H_2O \rightarrow H_2PO_3^- + 2H \quad (3)$$

$$Cu^{2+} + 2H_2PO_2^- + 2H_2O \rightarrow Cu + 2H_2PO_3^- + 2H^+ + H_2 \quad (4)$$

### 3.2 Effect of bonding temperature on bondability

Figure 3 exhibits the shear strength of joint bonded using Cu+Ag mixed nanoparticles (molar ratio 1 : 1) as a function of bonding temperatures. When the bonding temperature is 160°C, the shear strength of the joint is low (about 2 MPa). As the bonding temperature increased to 200°C, the shear strength is increased obviously (about 12 MPa). When the bonding temperature increased to 250–350°C, the strength is about 20 MPa. The small reduction of the joint strength may be related with slight oxidation of Cu nanoparticles, which need further study.

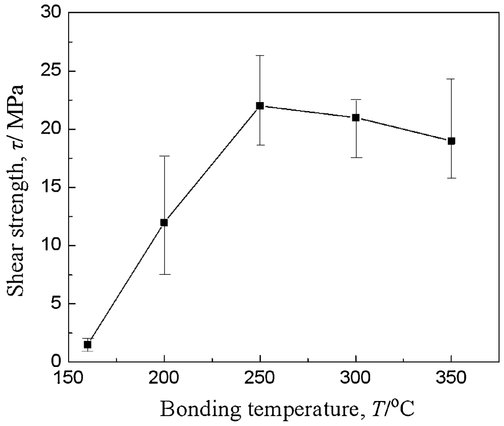

Fig. 3 Shear strength of joint bonded with Cu+Ag mixed nanoparticles (molar ratio 1 : 1) at different temperatures.

The fracture surfaces of the joints bonded using Cu+Ag mixed nanoparticles (molar ratio 1 : 1) at different temperatures are shown in Fig. 4. Different fracture microstructures are seen for the joints bonded at different temperatures. At the bonding temperature of 160°C, the Cu+Ag mixed nanoparticles are still encapsulated by polymers. No obvious sintering occurs, which lead to the low bonding strength. As the temperature is increased to 200–350°C, fracture surfaces show obvious ductile tearing of microstructure between the sintered nanoparticles, which is corresponded to the improvement of the joint strength.[15)] This result seems to show that strong joint is got when the nanoparticles are sintered together. It is reasonable to deduce that the interparticle bond between the sintered adjacent particles has a significant influence on the joint strength.

The X-ray diffraction (XRD) patterns of fracture microstructure of the joints bonded using mixed Cu+Ag nanoparticles at different temperatures are shown in Fig. 5. Peaks attributed to those of metallic Cu and Ag are detected. No

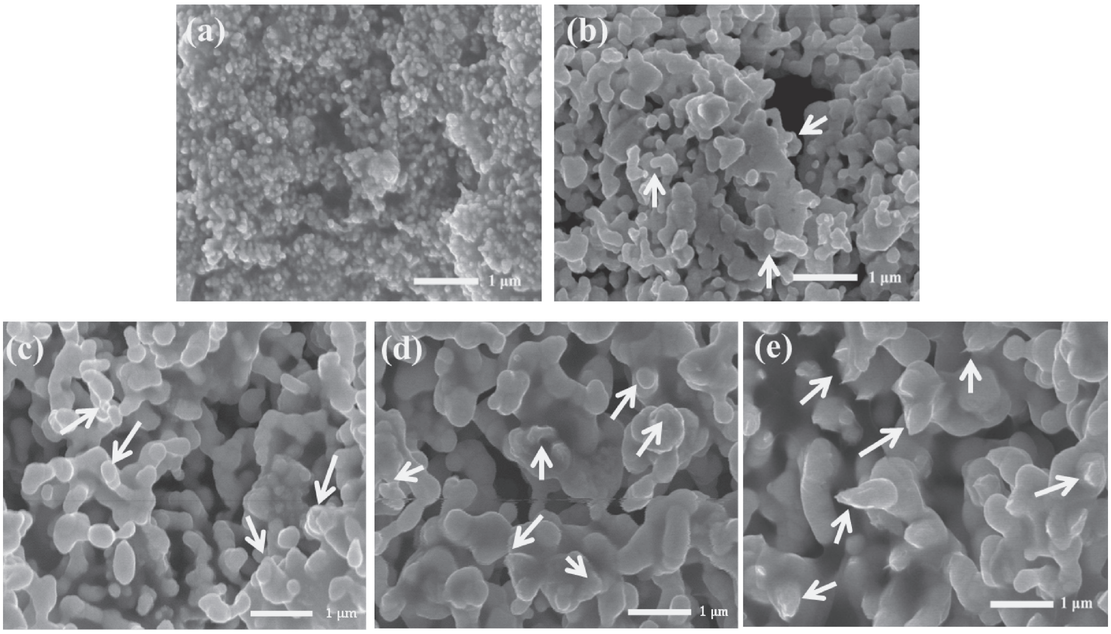

Fig. 4 SEM images of the fracture surface bonded with Cu+Ag mixed nanoparticles (molar ratio 1 : 1) at different temperatures. (a) 160°C. (b) 200°C. (c) 250°C. (d) 300°C. (e) 350°C. (Arrows show tearing of microstructure between the sintered nanoparticles.)

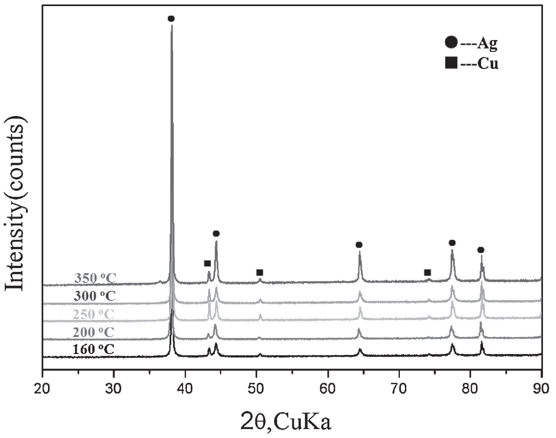

Fig. 5 XRD diffraction patterns of fracture surfaces of the joints boned using mixed Cu+Ag nanoparticles at different temperatures (bonding temperatures: 160–350°C).

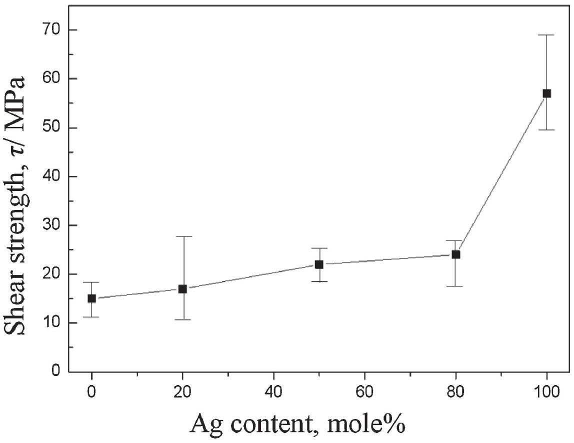

Fig. 6 Shear strength of joints bonded using Cu+Ag mixed nanoparticles with different Cu/Ag molar ratio (Cu, Cu4/Ag1, Cu1/Ag1, Cu1/Ag4, Ag).

obvious oxidation peak appears, which indicates that the polymer can protect most of the Cu nanoparticles from oxidation. It should be note that prevention of the oxidation of copper is important for the improvement the joint quality.[8)]

### 3.3 Effect of Cu content on bondability

Figure 6 shows the shear strength of the joint bonded using Cu+Ag mixed nanoparticles with different Cu/Ag molar ratio at 250°C under 5 MPa. Strong joint is got using Ag nanoparticles, which has shear strength about 55 MPa. However, with the increase of Cu content in the Cu+Ag mixed nanoparticles, the joint strength decreased to about 20 MPa. This result is obvious different from that sintering bonding process of copper wire and copper pad, in which the bondability is improved with the increasing of Cu content in Cu+Ag mixed nanoparticles.[12)] The difference is probably due to the difference of the base metal. Here, the base metal is the silver plated Cu bulks instead of oxygen free copper wires and foils. The strength bonded using Cu+Ag mixed nanoparticles is lower than that bonded using pure Ag nanoparticles. Figure 7 shows the corresponding fracture surfaces of the joint using Cu+Ag mixed nanoparticles with different Cu content. When using pure Cu nanoparticles as the bonding materials, few tearing of microstructure between the sintered nanoparticles are seen. The joint has a strength of 15 MPa. With the increase of the Ag content, more tearing of microstructure can be seen. When using pure Ag nanoparticles as the bonding materials, the tearing microstructures are obvious. This indicates that the addition of Cu nanoparticles has an adverse effect on the sintering of nanoparticles.

Figure 8 shows the representative cross sectional image and the element mapping map of the joint boned using Cu+Ag mixed nanoparticles (molar ratio 1 : 1) at 250°C under 5 MPa for 5 min. Cu nanoparticles which is mixed in the Ag nanoparticles can be detected. Many voids can be seen

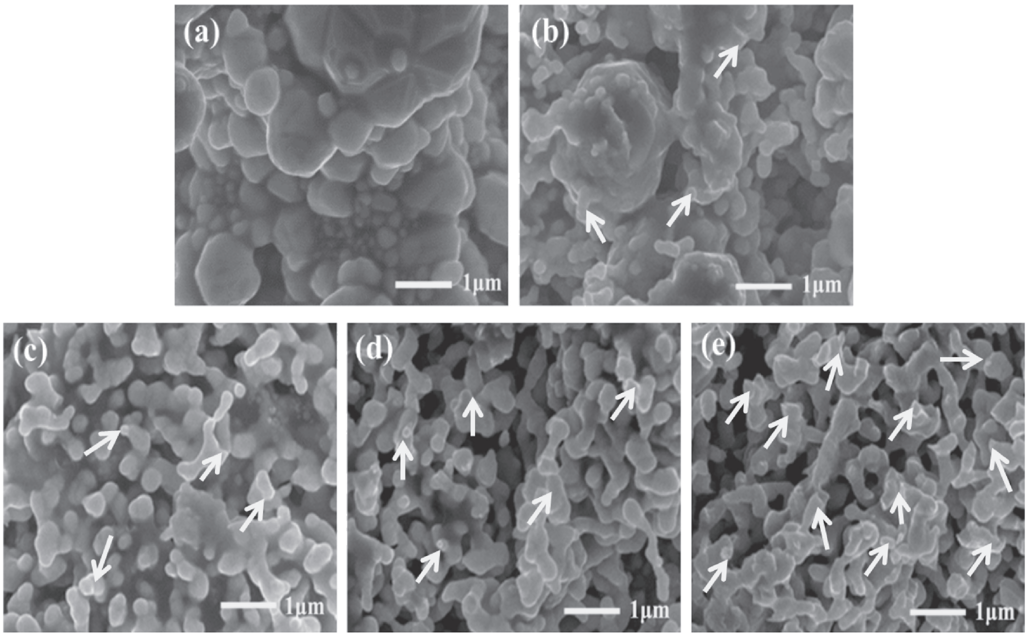

Fig. 7 SEM images of the fracture surface bonded with Cu+Ag mixed NPs (different Cu/Ag molar ratio). (a) Cu. (b) Cu4/Ag1. (c) Cu1/Ag1. (d) Cu1/Ag4. (e) Ag. (Arrows show tearing of microstructure between the sintered nanoparticles.)

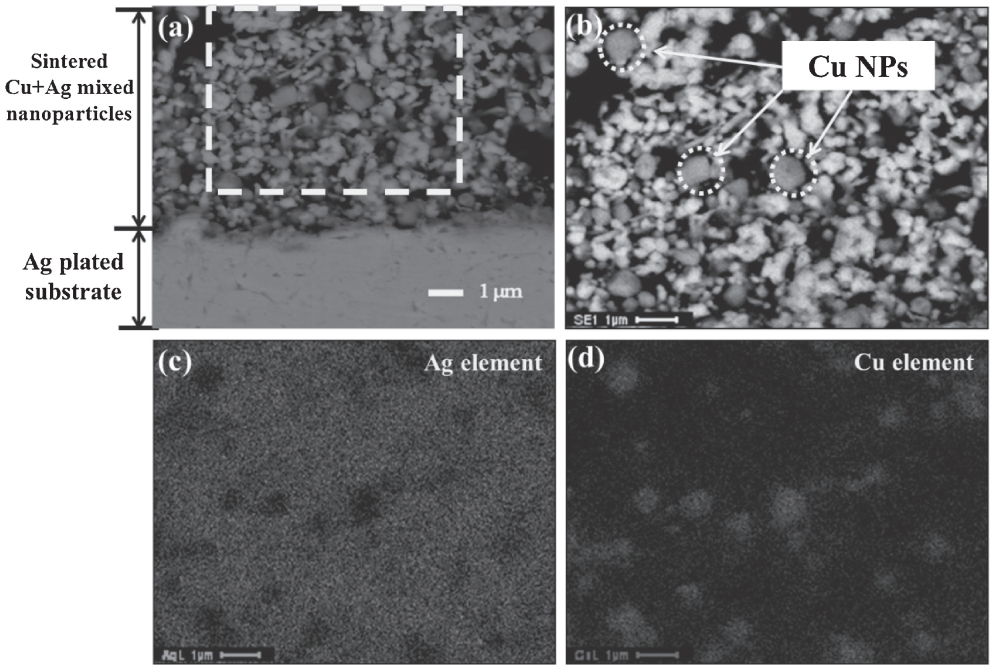

Fig. 8 Representative SEM images cross sectional image of the joint and the element mapping map.

around the Cu nanoparticles. As mentioned above, the Cu content has an adverse effect on the joint strength and this may due to the voids near the Cu nanoparticles. Figure 9 is the SEM images of fracture surface of joint bonded using Cu+Ag mixed nanoparticles. Based on the EDX spectra result, it is known that point A is the sintered Ag nanoparticles and point B is consisted of sintered Cu nanoaprticles. It is interesting that at the region consisted of Ag nanoparticles the tearing microstructures are obvious. No obvious tearing microstructures at the region consisted of Cu nanoparticles were seen. These fracture morphologies may indicate that the sintering between the Cu nanoparticles and the Ag nanoparticles is more difficult than that between Ag nanoparitlces. It is reasonable to assume that the fracture path is along the Cu nanoparticles, where lots of voids existed. Based on the above discussion, the possible schematics of the sintering behaviors of Cu+Ag mixed nanoparticles and possible crack path in the sintered Cu+Ag mixed nanoparticles are shown in Fig. 10. This illustrates that the Cu nanoparticles is the weak position and the crack path extend along the void around Cu nanoparticles. Due to these reasons, it is reasonable to deduce that the addiction of Cu nanoparticles to Ag nanoparticles will reduce the joint strength, which is consistent with the above experimental results.

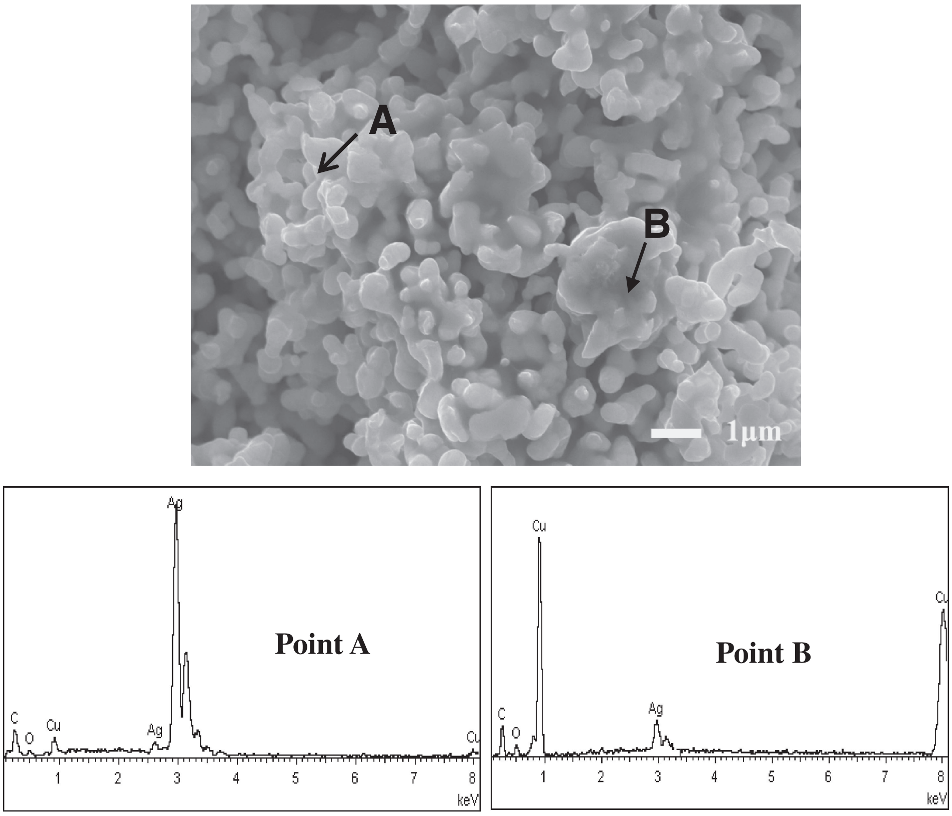

Fig. 9 SEM images of fracture surface of joint made using Cu+Ag mixed nanoparticles and the EDX spectra at point A and at point B.

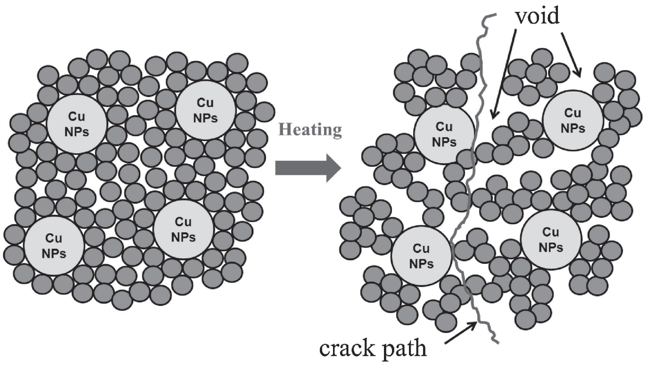

Fig. 10 Schematics of possible sintering behaviors and crack path in the sintered Cu+Ag mixed nanoparticles.

## 4. Conclusions

In summary, we have succeeded in the bonding of silver plated Cu bulks using Cu+Ag mixed nanoparticles. No obvious oxidation of Cu nanoparticles was detected in the fracture surfaces of the joint. The joints with shear strength about 20 MPa was formed at the bonding temperature above 250°C under 5 MPa using Cu+Ag mixed nanoparticles. The addition of Cu nanoparticles to Ag nanoparticles reduces the joint strength. This may due to the addition of Cu nanoparticles has an adverse effect on the sintering of nanoparticles and many voids exists around the Cu nanoparticles.

## Acknowledgement

This research was supported by the National Natural Science Foundation of China (Grant No. 51075232) and by Tsinghua University Initiative Scientific Research Program (Grant No. 2010THZ 02-1).

## REFERENCES

1) Y. Li, K. Moon and C. Wong: Science **308** (2005) 1419–1420.
2) K. Suganuma: Curr. Opin. Solid State Mater. Sci. **5** (2001) 55–64.
3) M. Abtew and G. Selvaduray: Mater. Sci. Eng. Rep. **27** (2000) 95–141.
4) H. Ogura, M. Maruyama, R. Matsubayashi, T. Ogawa, S. Nakamura, T. Komatsu, H. Nagasawa, A. Ichimura and S. Isoda: J. Electron. Mater. **39** (2010) 1233–1240.
5) Y. Zhou (ed.): *Microjoining and Nanojoining*, (Cambridge, 464 UK: CRC/Woodhead, 2008).
6) E. Ide, S. Angata, A. Hirose and K. F. Kobayashi: Acta Mater. **53** (2005) 2385–2393.
7) A. Hu, J. Y. Guo, H. Alarifi, G. Patane, Y. Zhou, G. Compagnini and C. X. Xu: Appl. Phys. Lett. **97** (2010) 153117.
8) Y. Jianfeng, Z. Guisheng, H. Anming and Y. N. Zhou: J. Mater. Chem. **21** (2011) 15981–15986.
9) Q. Cui, F. Gao, S. Mukherjee and Z. Gu: Small. **5** (2009) 1246–1257.
10) T. Morita, E. Ide, Y. Yasuda, A. Hirose and K. Kobayashi: JPN. J. Appl. Phys. **47** (2008) 6615–6622.
11) J. G. Bai and L. Guo-Quan: IEEE. Trans. Device. Mater. Reliab. **6** (2006) 436–441.
12) J. Yan, G. Zou, A. Wu, J. Ren, A. Hu and Y. N. Zhou: J. Electron. Mater. **41** (2012) 1886–1892.
13) Y. Sun and Y. Xia: Science **298** (2002) 2176–2179.
14) J. Yan, G. Zou, A. Wu, J. Ren, A. Hu and Y. Zhou: Scr. Mater. **66** (2012) 582–585.
15) A. Hasnaoui, H. Van Swygenhoven and P. M. Derlet: Science **300** (2003) 1550–1552.